MedCrave
Step into the World of Research
Journal of Analytical & Pharmaceutical research

Research Article
Open Access
CrossMark

# Kinetics of photocatalytic degradation of methylene blue dye in aqueous medium using ZnO nanoparticles under UV radiation

## Abstract

Environmental pollution caused by untreated effluents from Paper, textile, printing, and several other industries is of serious concern. These industries generate a tremendous amount of wastewater contaminated with harmful chemicals. Methylene blue dye finds important application in pharmaceuticals to treat methemoglobinemia: a rare blood disorder. However, while present in drinking water or food material, methylene blue (MB) dye is a serious health hazard as it is carcinogenic and non-biodegradable that can cause a threat to human health and environmental safety. Hence, there is a need to develop an environmental friendly, and efficient technology for removing MB from wastewater. The usual physical and chemical methods employed for the removal of dyes are less efficient, costlier, and generate solid waste with adverse environmental impact. In the present work, Zinc oxide (ZnO) nanoparticles were synthesized by hydrolysis and oxidative method. As-synthesized ZnO powder was characterized using X-ray diffraction, and UV visible spectroscopic techniques. Photocatalytic degradation of methylene blue dye, catalyzed by as-synthesized ZnO nanoparticles, has been carried out in aqueous medium under UV radiation. The effects of operating parameters, such as amount of ZnO catalysts, pH, and initial concentration of dye on MB degradation, were investigated. The photo-catalytic degradation of MB was found to follow the *pseudo-first-order* kinetic model. Using ZnO optimum load 250 $mgL^{-1}$, solution pH 10, the degradation of 20 $mgL^{-1}$ MB was 85% at 3 hrs. Keeping in view its low cost, and high photocatalytic efficacy, the nanosize ZnO can be used for a large scale treatment of wastewater contaminated with methylene blue dye as pollutant.

**Keywords:** nanoparticles, methylene blue, kinetic, photocatalytic, degradation

Volume 12 Issue 1 - 2023

Harife Etay,[1] Ashok Kumar,[2] O.P.Yadav[3]
[1]Chemistry Department, Haramaya Univeresity, Ethiopia
[2]Chemistry Department, RKSD (PG) College, India
[3]Chemistry Department, CCS Haryana Agricultural University, India

**Correspondence:** O.P.Yadav, Chemistry Department, CCS Haryana Agricultural University, Hisar-125004, India, Tel +91-8059602660, Email yadavo02@yahoo.com

**Received:** February 20, 2023 | **Published:** March 02, 2023

## Introduction

Methylene blue, a thiazine dye, is used in pharmaceuticals as a medication to treat methemoglobinemia: a rare blood disorder, by converting ferric iron in hemoglobin to ferrous iron. Partricularly, it is used to treat methemoglobin levels that are greater than 30% or in which there are symptoms despite oxygen therapy. Methylene blue (MB) dye is also a highly consumed material in the dye, textile, and paper industries.[1,2] Since MB is highly toxic, carcinogenic and non-biodegradable, its presence in wastewater can cause severe threat to human health as well as environmental safety. Ingestion of MB in human body through contaminated drinking water or food, can cause irritation of skin, mouth, and stomach; nausea, headache, vomiting, anemia & diarrhea.[3] Therefore, the pre-treatment of wastewater contaminated with MB dye becomes necessary for maintaining the quality of water and its safer use.[4,5] Wen et al.[6] developed a potentiometric method for its use in pharmaceuticals for quantitative determination of MB in injections.

Untreated effluents from paper, dying, printing, and textile industries generate a tremendous amount of wastewater containing several health hazard chemicals. The usual methods employed for removing organic pollutants from wastewater include adsorption/biosorption[7-9], coagulation/flocculation,[10,11] phytoremediation,[12,13] biodegradation,[14-16] liquid-liquid extraction,[17] electrocoagulation,[18,19] ultrafilttration,[20,21]and nanofiltration.[22,23] These methods are less efficient, costlier, and generate solid waste which requires secondary treatment.[24]

In the recent years, heterogeneous photo-catalytic degradation of recalcitrant organic compounds using semiconducting nanomaterial has received increased attention because of its high efficiency, cost-effectiveness, and environmental friendly process for treating wastewater.[25-27] Zinc oxide (ZnO), due to its unique piezoelectric and ferromagnetic properties, has been used in the development of several devices of great practical use.[28] Based on piezoelectric property of ZnO there are optoelectronic devices such as light emitting diodes (LEDs), solar cells,[29] optical fibres etc. Ferromagnetic property of ZnO has been exploited in producing spintronics used in storing large data. Zinc oxide is also used in anti-UV radiation cosmetics, gas sensors, cancer detecting biosensors, and degradation of organic toxins.[30] Zinc oxide due to its low cost, non-toxic nature, good stability, and high performance efficiency in photocatalysis have also drawn increasing attention for its use in the treatment of wastewater.[31-33] Zinc oxide with band gap energy (3.37 eV), upon photexcitation in aqueous medium under UV radiation, generates hole ($h^+$) with high oxidation potential. These reactive holes through several oxidative steps enable degradation of organic pollutants to generate simple non-toxic products such as $CO_2$, $H_2O$ etc.

Acosta-Silva et al.[34] used $TiO_2$-decorated Santa Barbara Amorphous (SBA-15) mesoporous material for photocatalytic degradation of methylene blue (MB). Alamdari et al.[35] green synthesized zinc oxide nanoparticles mediated by *Sambucus ebulus* leaf extract and used this material for photocatalytic degradation of methylene blue dye in the aqueous medium. The present work was carried out to investigate the effects of operational parameters such as catalyst load, solution pH, and dye initial concentration, on the kinetic of photocatalytic degradation of methylene blue under UV radiation.

## Material and methods

### Chemicals

Zinc chloride ($ZnCl_2$; MW:136.32 g $mol^{-1}$; hydrochloric acid (HCl, MW:36.5 g $mol^{-1}$) were from Blulux Laboratories. Sodium hydroxide (NaOH, MW: 40 g $mol^{-1}$, 98% pure), and Methylene blue ($C_{16}H_{18}ClN_3S$, MW: 319.85 g $mol^{-1}$) were procured from Breckland Scientific Supplies. The structural formula of methylene blue is shown in Figure 1.

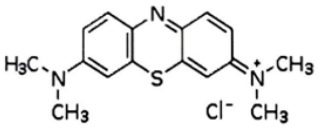


**Figure 1** The structural formula of methylene blue.

### Methods

**Preparation of ZnO:** Zinc oxide (ZnO) nanoparticles were prepared using hydrolysis and oxidation process. Typically, 0.M $ZnCl_2$ solution taken in a glass beaker was mixed, dropwise, with 1M NaOH solution and the mixture was stirred until the pH of the solution reached to 12. White precipitates thus obtained were thoroughly washed with distilled water. The product was dried at 120 $^0$C, and then calcined at 600°C for 3 hrs to get crystalline ZnO powder.[36]

**X-ray diffraction study:** The X-ray diffraction pattern of as-synthesized ZnO powder was recorded using an X-ray diffractometer (BRUKERD8 Advance XRD, AXS GMBH, Karisruhe, West Germany) equipped with Cu target for generating CuKα radiation (wavelength: 1.5406 A°). The applied accelerating voltage, and the current were 40 kV, and 30 mA, respectively. The instrument was operated under step scan type with step time, and 2θ degree as 1 sec, and 0.020$^0$, respectively over 2θ range of 4° to 64°.

**UV-visible absorption study:** The UV-Visible diffuse absorption spectrum was recorded using a spectrophotometer (Perkin Elmer SP65). Typically, 0.2% aqueous dispersion (w/v) of ZnO was taken in a quartz tube, and the absorption spectra was recorded over 200-800 nm. The wavelength (nm) against the absorption peak maxima was recorded.

**Photocatalytic degradation study:** Photocatalytic degradation of methylene blue (MB) in its aqueous solution under UV radiation was carried out at ambient temperature. Typically, a known amount of the photocatalyst powder was thoroughly mixed with the MB dye solution of given concentration in a pyrex reactor tube. It was then put under UV lamp (Philips), predominantly emitting radiation at 365 nm. The UV lamp (with definite power 12 W; 230 Volts and 50 Hz frequency) was positioned parallel to the reactor tube at a distance of 6 cm. The desired pH of the reaction mixture was achieved by adding dropwise 0.1M NaOH or 0.1M HCl solution, and the reaction mixture was stirred at 3000 rpm to eliminate the external mass transfer effect. Before irradiating under UV light, the reaction mixture was magnetically stirred under dark for 15 minutes to establish adsorption/desorption equilibrium of methylene blue. Five ml each of reaction mixture was withdrawn after every 10 minutes, centrifuged at 4000 rpm for 20 minutes, and the concentration of methylene blue in the supernatant liquid was determined, spectrophotometrically, by recording absorbance at 665 nm.[37]

The percentage degradation of MB was calculated using equation 1.

$$\text{Degradation (\%)} = (C_0 - C_t)/C_0 \times 100 \quad (1)$$

Where, $C_o$ and $C_t$ are the concentrations dye in solution at the initial stage, and at time t, respectively.

## Results and discussion

### XRD analysis

The X-ray diffraction pattern of as-synthesized ZnO powder (Figure 2) depicting intense and narrow peaks indicates its crystalline nature. The diffraction peaks appearing at 2θ = 31.86, 34.54, 36.32, 47.62, 56.66 and 62.96 correspond to crystal planes (100), (002), (101), (102), (110) and (103) respectively, suggest the hexagonal wurtzite structure of the ZnO powder, and the same conforms with the JCPDS card, and other reports appeared in the literature.[38] Non-appearance of additional diffraction peaks, due to any foreign material, ensured the purity of the prepared ZnO powder.

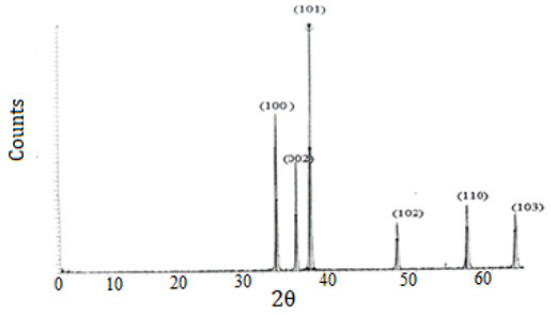


**Figure 2** The X-ray diffraction pattern of as-synthesized ZnO powder.

The average crystallite size of ZnO was obtained using Scherer formula[39] represented by Eqn. 2.

$$D = [K\lambda/(\beta\cos\theta)] \quad (2)$$

Where, D is the crystallite size in nm, K is the shape factor constant, taken as 0.94, β is the full width at half maximum (FWHM), in radians, for the most intense diffraction peak (at 2θ= 36.32) that corresponds to ZnO crystal plane (101), and λ is the wavelength of the X-ray (0.15406 nm), and θ represents the Bragg's angle. The values of β, and crystallite size of ZnO thus obtained were: 3.7x10$^{-3}$ radians, and 41.2 nm, respectively.

### UV/Visible Absorption Spectra

The UV/visible absorption spectrum of 0.2% ZnO aqueous dispersion (w/v) presented in Figure 3, exhibited the maximum absorption wavelength as 360 nm. The band gap energy of as-synthesized ZnO was obtained[40] using Eqn. 3.

$$E_{eV} = 1240/\lambda \quad (3)$$

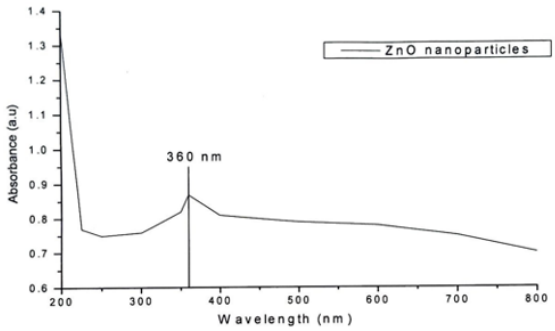


**Figure 3** UV-Visible diffuse absorption spectrum of Zinc oxide (ZnO) photocatalyst (absorption wavelength: 360 nm).

**Citation:** Etay H, Kumar A, Yadav OP. Kinetics of photocatalytic degradation of methylene blue dye in aqueous medium using ZnO nanoparticles under UV radiation. *J Anal Pharm Res.* 2023;12(1):32–37. DOI: 10.15406/japlr.2023.12.00421

Where, $E_{eV}$ represents band gap energy in electron volts, and λ is absorption wavelength in nm. The band gap energy thus calculated for synthesized ZnO nanoparticles was 3.44 eV.

## Kinetics of photocatalytic degradation

Batch experiments were performed for studying photocatalytic degradation of methylene blue (MB). To achieve maximum removal of MB from its aqueous solution, efforts were made to explore the required optimum catalyst load as well as the solution pH.

**Effect of photocatalyst load:** Plots of methylene blue percent degradation as a function of reaction time, using varying ZnO load, and MB initial concentration 20 $mgL^{-1}$, under UV radiation are shown in Figure 4. It was observed that as the catalyst load was raised from 50 to 250 $mgL^{-1}$, degradation of MB also increases till an optimum catalyst load (250 mg/L) was reached. But, upon further increasing the catalyst load to 300 $mgL^{-1}$, the photocatalytic degradation of MB is decreased. The observed increase in MB degradation upon raising the catalyst load upto the optimum value 250 $mgL^{-1}$ could be because of the increasing availability of active sites on the photocatalyst surface, and an increasing number of dye molecules adsorbed on the surface of the catalyst.[41] It leads to an increase in the number of photo generated highly reactive oxidant holes ($h^+$), hydroxyl, and superoxide radicals within the aqueous medium, which enable higher photocatalytic degradation of MB through a series of intermediate oxidative steps. However, when the concentration of ZnO catalyst was further increased above the limiting catalyst load (250 $mgL^{-1}$), the degradation of MB was lowered due to (a) increasing interception or scattering of UV radiation by enhanced ZnO particle density, and (b) the decreasing catalyst's specific surface area due to tendency of ZnO particles agglomeration at higher catalyst load. The percent removal of methylene blue dye from its 20 mg $L^{-1}$ solution was as high as 80% at the end of 200 min.

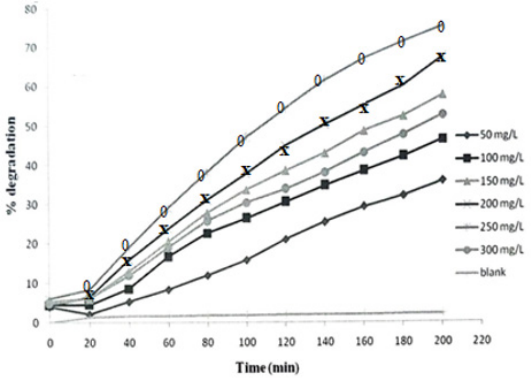


**Figure 4** Plots of percent degradation of 20$mgL^{-1}$ methylene blue (MB) under UV radiation as a function of time at varying ZnO catalyst load, and a fixed pH 10.

**Photocatalyst load dependent degradation kinetic:** Photocatalyst load dependent kinetic of methylene blue (MB) degradation behavior was examined in the light of *pseudo first order* kinetic model that can be represented by equation (4):

$$\ln(C_0/C_t) = k.t \quad (4)$$

Where, $C_o$ and $C_t$ represent MB concentrations at initial stage (zero time) and at time t, respectively. Plots of $\ln(C_0/C_t)$ versus time (t) for degradation of MB in its 20 $mgL^{-1}$ aqueous solution at varying ZnO load are shown in Figure 5. The observed linearity in these plots proves the applicability of the *pseudo first order* kinetic model for the photocatalytic degradation of MB in aqueous medium over the studied range of catalyst load. The rate constant (k) for MB degradation at any catalyst (ZnO) load, was obtained from the slope of the corresponding plot. The half-life time ($t_{1/2}$) of MB in solution was obtained using Eqn. 5,

$$\text{Half-life time } (t_{1/2}) = 0.693/\ k \quad (5)$$

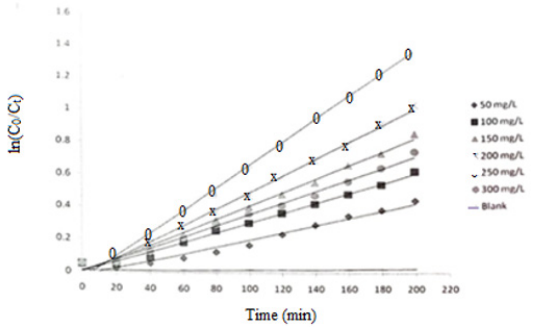


**Figure 5** Plots of $\ln C_0/C_t$ as a function of reaction time (min) at varying ZnO load ($mgL^{-1}$); (MB initial concentration 20 $mgL^{-1}$, and optimum pH 10.

The degradation rate constant k, and $t_{1/2,}$ at varying catalyst loads thus obtained, are recorded in Table 1, and also shown as plots of catalyst load versus k, and $t_{1/2}$ in Figures 6A&6B, respectively. Photocatalytic degradation rate of MB gradually increases upon raising the catalyst (ZnO) amout till the optimum ZnO load 250 $mgL^{-1}$ is reached where the maximum rate of dye degration $6.23x10^{-3}$ $min^{-1}$, while at a higher catalyst load (300 $mgL^{-1}$) it decreases to 5.97 $x10^{-3}$ $min^{-1}$. There is an obvious opposite trend in MB half-life time which decreases from 385.0 to 111.2 min till the optimum catalyst load is reached, and then it increases to 116.1 min at higher ZnO load.

**Table 1** *Pseudo first-order* photocatalytic degradation rate constant (k) ($min^{-1}$), and MB half-life time ($t_{1/2}$) (min) in solution at varying photocatalyst (ZnO) load under UV radiation

| [ZnO] ($mgL^{-1}$) | $kx10^{+3}$ ($min^{-1}$) | $t_{1/2}$ (min) |
|---|---|---|
| 50 | 1.80 | 385.0 |
| 100 | 2.94 | 235.7 |
| 150 | 3.94 | 175.9 |
| 200 | 4.89 | 141.7 |
| 250 | 6.23 | 111.2 |
| 300 | 5.97 | 116.1 |

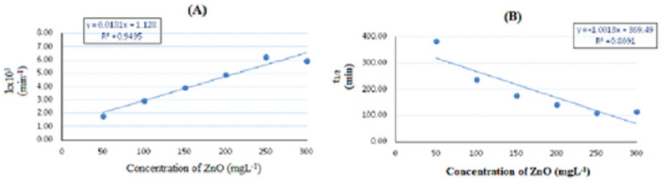


**Figure 6** (A) Plot of methylene blue photocatalytic degradation rate constant k($min^{-1}$) versus concentration of ZnO. (B) Plot of methylene blue half-life time $t_{1/2}$ (min) versus concentration of ZnO. (MB dye initial concentration 20 $mgL^{-1}$, optimum pH 10; under UV irradiation).

**Effect of pH**: Besides the need of optimizing the catalyst load, discussed above, for obtaining maximum degradation of organic pollutant such as MB, selection of optimum pH of the reaction medium is also important. It is because the pH affects both the nature and intensity of net electrical charge on the catalyst surface, and also the net charge on the substrate (MB) molecules. Both these factors affect the extent of adsorption of dye molecules at the photocatalyst (ZnO) guided by the level of ion-ion attraction or repulsion, which in turn affects the rate of photocatalytic molecular decomposition of the substrate (MB).[42] Plots of percent photocatalytic degradation of MB as a function of reaction

time, at varying pH of aqueous medium, is shown in Figure 7. Upon raising the solution pH from 7 to 10, photocatalytic degradation of MB increased from 48 % to 85 % at 3 hrs, but upon raising the pH at 11, MB degradation decreased to 70 %. With MB intial concentration 20 $mgL^{-1}$, optimum catalyst load 250 $mgL^{-1}$, and pH 10, maximum 85% degradation of MB was achieved under the UV radiation. The observed increasing MB degradation at higher pH (till the optimum pH) could be due to the increasing hydroxyl ions in aqueous medium which upon reacting with the photogenerated holes ($h^+$) generate more hydroxyl radicals ($^{\cdot}OH$) needed for photocatalytic degradation of MB. The increase in MB degradation at higher pH may also be described in terms of variations of surface charge properties of the photocatalyst. Zinc oxide has point of zero charge (pzc) pH = 9.0 (pzc) pH = 9.0.[43-44]

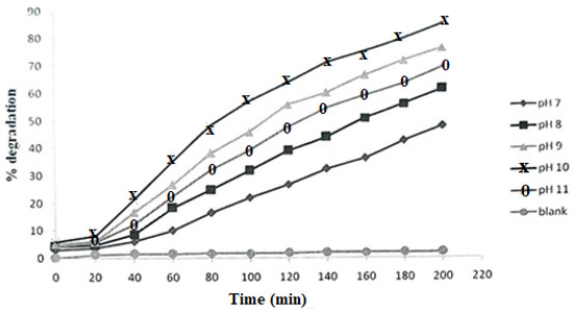


**Figure 7** Plots of percent degradation of MB as a function of time at varying solution pH under UV radiation (MB initial concentration 20 $mgL^{-1}$)

At a pH higher than pzc, the catalyst surface acquires negative charge and the reverse occurs at pH less than pzc. Since MB is a cationic dye, it obviously adsorbs more MB molecules at the negatively charged ZnO surface at higher pH. Further, since MB adsorption at the catalyst surface is a pre-requirement for photocatalytic reaction, the dye degradation would obviously be faster at higher pH. However, the decrease in MB degradation at still higher pH (=11) could be due to alkaline dissolution of ZnO.[45,46]

pH dependent degradation kinetic: The pH dependent MB photocatalytic degradation kinetic was studied following the *pseudo first order* kinetic model. Plots of $\ln(C_0/C)$ as a function of time (min) at varying solution pH under UV radiation are shown in Figure 8. Photocatalytic degradation rate constant, k ($min^{-1}$), and MB half-life, $t_{1/2}$ (min) at varying pH of solution are given in Table 2, and the plot of MB photocatalytic degradation rate constant k($min^{-1}$) versus solution pH is shown in Figure 9A, and plot of methylene blue half-life time $t_{1/2}$ (min) versus solution pH is given in Figure 9B. The maximum degradation rate of MB at the optimum pH=10 was found to be $7.02x10^{-3}min^{-1}$ with MB half life time ($t^{1/2}$) 98.7 min.

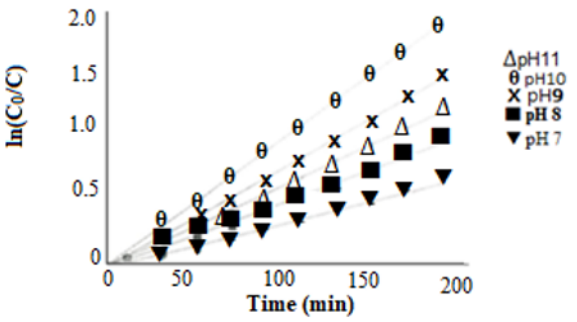


**Figure 8** Plots of $\ln(C_0/C)$ as a function of time (min) at varying solution pH under UV radiation [MB initial concentration ($C_0$): 20 $mgL^{-1}$; catalyst load : 250 $mgL^{-1}$].

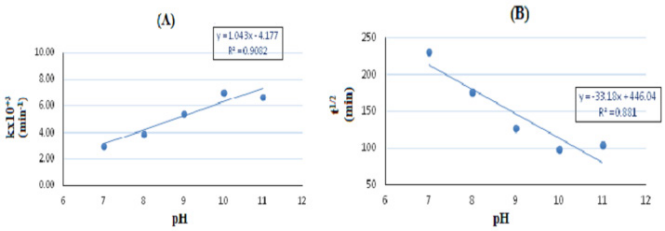


**Figure 9** (A) Plot of methylene blue (MB) photocatalytic degradation rate constant k($min^{-1}$) versus solution pH. (B) Plot of methylene blue half-life time $t_{1/2}$ (min) versus solution pH. [MB initial concentration ($C_0$): 20 $mgL^{-1}$, catalyst load: 250 $mgL^{-1}$].

**Table 2** Pseudo first order photocatalytic degradation rate constant, k, and MB half-life, ($t_{1/2}$) at varying pH of reaction mixture under UV radaiation

| pH | kx10*3 ($min^{-1}$) | $t_{1/2}$ (min) |
|---|---|---|
| 7 | 3.00 | 231.0 |
| 8 | 3.93 | 176.3 |
| 9 | 5.43 | 127.2 |
| 10 | 7.02 | 98.7 |
| 11 | 6.67 | 103.9 |

**Effect of methylene blue concentration:** To explore the effect of substrate (MB) initial concentration on its degradation, experiments were performed by varying initial concentrations MB from 20 to 100 $mgL^{-1}$. The plots of MB percent degradation as a function of time (min) (optimum catalyst load: 250 $mgL^{-1}$; pH: 10), using varying initial concentrations of MB, are shown in Figure 10. The percent degradation of MB was found to decrease with its increasing initial concentration. It could be because for the given catalyst load, with increasing concentration of MB, the availability of surface active site per dye molecule decreases. Besides it, at higher dye concentration, due to the absorption of some UV radiation by dye molecules in solution, the intensity of photons reaching at the catalyst surface diminishes leading to a decreased degradation rate of methylene blue.

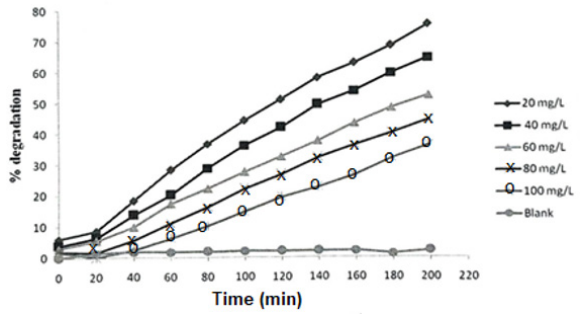


**Figure 10** Percent degradation of MB dye under UV radiation as a function time using varying initial concentration ($C_0$) of dye[optimum ZnO load: 250 $mgL^{-1}$, and pH=10].

Dye concentration dependent degradation kinetic: The plots of $\ln(C_0/C)$ as a function of time (optimum catalyst load 250 $mgL^{-1}$, and pH 10) using varying concentrations of MB, are shown in Figure 11. The observed linear plots of $\ln(C_0/C)$ versus time, proves the applicability of *pseudo first order* kinetic model for dye degradation over its different studied intial concentrations. Values of MB photocatalytic degradation rate constant (k), and MB half-life time ($t_{1/2}$) in solution, using varying initial concentration ($C_0$) of MB, are given in Table 3. Plots of degradation rate constant (k), and MB half-life ($t_{1/2}$), each as a function of MB intial concentration ($C_0$), are shown in Figure 12A&12B, respectively. Whereas, the dye degradation rate

**Citation:** Etay H, Kumar A, Yadav OP. Kinetics of photocatalytic degradation of methylene blue dye in aqueous medium using ZnO nanoparticles under UV radiation. *J Anal Pharm Res.* 2023;12(1):32–37. DOI: 10.15406/japlr.2023.12.00421

decreases with increasing initial concentration ($C_0$) of MB, the dye half-life time ($t_{1/2}$) in solution has the reverse trend.

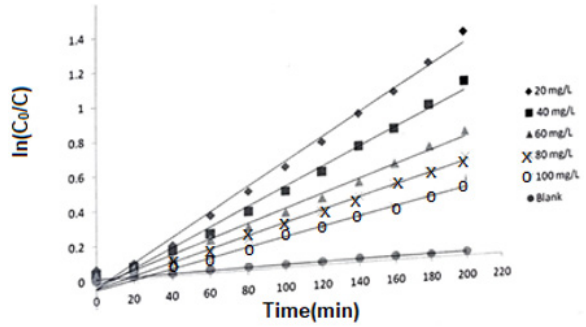


**Figure 11** Plots of $ln(C_0/C)$ as a function of time (min) at different initial concentration ($C_0$) of MB (optimum ZnO load: 250 $mgL^{-1}$, and pH: 10).

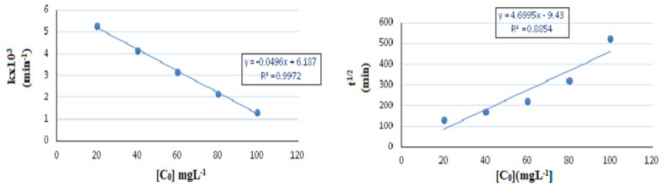


**Figure 12** (A) Plot of degradation rate constant, k ($min^{-1}$) versus MB intial concentration ($C_0$). (B) Plot of half-life ($t_{1/2}$) versus MB intial concentration ($C_0$) (optimum load of ZnO : 250 $mgL^{-1}$, and pH = 10).

**Table 3** Photocatalytic degradation rate constants k ($min^{-1}$), and half-life $t_{1/2}$(min) of MB in solution at different initial concentrations ($C_0$) of MB

| MB initial concentration ($C_0$) ($mgL^{-1}$) | Degradation rate constant $kx10^3$($min^{-1}$) | MB half-life time $t_{1/2}$ (min) |
|---|---|---|
| 20 | 5.29 | 131.0 |
| 40 | 4.14 | 167.4 |
| 60 | 3.15 | 220.0 |
| 80 | 2.17 | 319.3 |
| 100 | 1.32 | 525.0 |

## Conclusion

Zinc oxide (ZnO) nanoparticles have been prepared and used as catalyst in studying kinetics of photocatalytic degradation of methylene blue (MB) dye in aqueous medium under UV radiation. The efficiency of dye degradation was found to increase with increasing catalyst load as well pH of solution upto a limiting value in each case. But the degradation of MB decreased with increasing dye initial concentration over its studied range. The photocatalytic degradation of MB well fits the *pseudo-first-order* kinetic model. Under the optimum conditions of catalyst load: 250 $mgL^{-1}$, and pH: 10, the dye degradation rate under UV radiation was $5.29x10^{-3}$ $min^{-1}$, and the maximum 85% degradation/ decolourization of MB could be achieved in three hours. Considering the low cost of as-synthesized zinc oxide (ZnO) catalyst, and its good photo-catalytic efficiency, it can be recommended for a large scale treatment of wastewater contaminated with methylene blue dye as pollutant.

## Acknowledgments

None.

## Conflicts of interest

There is no conflicts of interest.

## References

1. Derakhshan Z, Baghapour MA, Ranjbar M, et al. Adsorption of methylene blue dye from aqueous solutions by modified pumice stone: Kinetics and equilibrium studies. *Health Scope*. 2013;2:136–144.
2. Han TH, Khan MM, Kalathil S, et al. Simultaneous enhancement of methylene blue degradation and power generation in a microbial fuel cell by gold nanoparticles. *Ind Eng Chem Res*. 2013;*52*:8174–8181.
3. Khan I, Saeed K, Zekker I, et al. Review on methylene blue: Its properties, uses, toxicity and photodegradation. *Water*. 2022; 14(2):242.
4. Zamel D, Hassanin AH, Ellethy R, et al. Novel bacteria–immobilized cellulose acetate/poly(ethylene oxide) nanofibrous membrane for wastewater treatment. *Sci Rep*. 2019;9:18994.
5. Thabede PM, Shooto ND, Naidoo EB. Removal of methylene blue dye and lead ions from aqueous solution using activated carbon from black cumin seeds. *S Afr J Chem Eng*. 2020;33:39–50.
6. Wen ML, Zhao YB, Chen X, et al. Potentiometric sensor for methylene blue based on methylene blue–silicotungstate ion association and its pharmaceutical applications. *J Pharmaceut Biomed Anal*. 1999;18(6):957–961.
7. Regunton PCV, Sumalapao DEP, Villarante NR. Biosorption of methylene blue from aqueous solution by coconut (Cocos nucifera) shell–derived activated carbon–chitosan composite. *Orient J Chem*. 2018;34:115–124.
8. Wang Z, Gao M, Li X, et al. Efficient adsorption of methylene blue from aqueous solution by graphene oxide modified persimmon tannins. *Mater Sci Eng C*. 2020;108:110196.
9. Siqueira TCA, da Silva IZ, Rubio AJ, et al. Sugarcane bagasse as an efficient biosorbent for methylene blue removal: Kinetics, isotherms and thermodynamics. *Int J Environ Res Public Health*. 2020;17(2):526.
10. Lau YY, Wong YS, Teng TT, et al. Degradation of cationic and anionic dyes in coagulation–flocculation process using bi–functionalized silica hybrid with aluminum–ferric as auxiliary agent. *RSC Adv*. 2015;5:34206–34215.
11. Liu J, Li P, Xiao H, et al. Understanding flocculation mechanism of graphene oxide for organic dyes from water: experimental and molecular dynamics simulation. *AIP Adv*. 2015;5(11):117151.
12. Tan KA, Morad N, Ooi JQ. Phytoremediation of methylene blue and methyl orange using *Eichhornia Crassipes*. *Int J Environ Sci Dev*. 2016;7(10):724–728.
13. Imron MF, Kurniawan SB, Soegianto A, et al. Phytoremediation of methylene blue using duckweed (*Lemna minor*). *Heliyon*. 2019;5(8):e02206.
14. Eslami H, Sedighi KS, Salehi F, et al. Biodegradation of methylene blue from aqueous solution by bacteria isolated from contaminated soil. *J Adv Environ Health Res*. 2017;5(1):10–15.
15. Kilany M. Isolation, screening and molecular identification of novel bacterial strain removing methylene blue from water solutions. *Appl Water Sci.*, 2017;7(7):4091–4098.
16. Van Der Maas, Da Silva, Aruana Rocha, et al. The degradation of methylene blue dye by the strains of *pleurotus sp*. With potential applications in bioremediation processes. *Rev Ambient Agua*. 2018;13(4):e2247.
17. El–Ashtoukhy ESZ, Fouad YO. Liquid–liquid extraction of methylene blue dye from aqueous solutions using sodium dodecylbenzenesulfonate as an extractant. *Alexandria Engineering Journal*. 2015;54(1):77–81.
18. Mahmoud MS, Farah JY, Farrag TE. Enhanced removal of methylene blue by electrocoagulation using iron electrodes. *Egypt J Pet*. 2013;22(1): 211–216.

19. Tir M, Moulai Mostefa, Nedjhioui M. Optimizing decolorization of methylene blue dye by electrocoagulation using taguchi approach. *Desalin Water Treat.* 2015;55(10):2705–2710.

20. Khosa MA, Shah SS, Nazar MF. Application of micellar enhanced ultrafiltration for the removal of methylene blue from aqueous solution. *J Dispers Sci Technol*. 2011;32(2):260–264.

21. Kim S, Yu M, Yoon Y. Fouling and retention mechanisms of selected cationic and anionic dyes in a Ti3C2Tx MXene–Ultrafiltration Hybrid System. *ACS Appl Mater Interfaces*. 2020;12(14):16557–16565.

22. Cheng S, Oatley DL, Williams PM, et al. Characterisation and application of a novel positively charged nanofiltration membrane for the treatment of textile industry wastewaters. *Water Res.* 2012;46(1):33–42.

23. Kong G, Pang J, Tang Y, et al. Efficient dye nanofiltration of a graphene oxide membrane: Via combination with a covalent organic framework by hot pressing. *J Mater Chem A*. 2019;7(42):24301–24310.

24. Crini G, Lichtfouse E. Advantages and disadvantages of techniques used for wastewater treatment. *Environ Chem Lett*. 2019;17(1):145–155.

25. Kiros G, Yadav OP, Taddesse A. Effect of Ag–N co–doping in nanosize $TiO_2$ on photocatalytic degradation of methyl orange Dye. *J Surf Sci Technol.* 2013;29:1–14.

26. Achamo T, Yadav OP. Removal of 4–Nitrophenol from water using Ag–N–P tridoped $TiO_2$ by photocatalytic oxidation technique. *Anal Chem Insights.* 2016;11:29–34.

27. Madkour M, Allam OG, Nazeer A, et al. $CeO_2$–based nanoheterostructures with p–n and n–n heterojunction arrangements for enhancing the solar–driven photodegradation of rhodamine 6G dye. *J Mater Sci Mater Electron*. 2019;30:10857–10866.

28. Özgür Ü, Alivov YI, Liu C, et al. A comprehensive review of ZnO materials and devices. J Appl *Phys*. 2005;98(4):41301.

29. Quintana M, Edvinsson T, Hagfeldt A, et al. Comparison of dye–sensitized ZnO and $TiO_2$ solar cells: studies of charge transport and carrier lifetime. J Phys *Chem C*. 2007;111(2):1035–1041.

30. Krishnamoorthy S, Iliadis A, Bei T, et al. An interleukin–6 ZnO/$SiO_2$/Si surface acoustic wave biosensor. *Biosens Bioelectron.* 2008; 24(2):313–318.

31. Marto J, Marcos PS, Trindade T, et al. Photocatalytic decolouration of orange II by ZnO active layers screen–printed on ceramic tiles. *J Hazar Mater.* 2009;163(1):36–42.

32. Dutta M, Basak D. A novel and simple method to grow beaded nanochains of ZnO with superior photocatalytic activity. *Nanotechnol.* 2009;20(47):475602.

33. Balcha A, Yadav OP, Dey T. Photocatalytic degradation of methylene blue dye by zinc oxide nanoparticles obtained from precipitation and sol–gel methods. *Envir Sci Pollution Res.* 2016;23(24):25485–25493.

34. Acosta–Silva YJ, Nava R, Hernández–Morales V, et al. Methylene blue photodegradation over titania–decorated SBA–15. *Appl Catal B: Environmental*. 2011;110(2):108–117.

35. Alamdari S, Ghamsari MS, Lee C, et al. Preparation and characterization of zinc Oxide nanoparticles using leaf extract of *Sambucus ebulus*. *Appl Sci*. 2020;10(10):3620.

36. Dongwoon J. Synthesis and characterizations of transition metal–doped ZnO. *J solid state sci*. 2010;12(4):466–470.

37. Mekasuwandumrong O, Pawinrat P, Praserthdam P, et al. Effects of synthesis conditions and annealing post–treatment on the photocatalytic activities of ZnO nanoparticles in the degradation of methylene blue dye. *Chem Eng J.* 2010;164(1):77–84.

38. Hayata K, Gondal MA, Khaled MM, et al. Nano ZnO synthesis by modified sol–gel method and its application in heterogeneous photocatalytic removal of phenol from water. *Applied Catalysis A: General.* 2011;393(1–2):122–129.

39. Zheng M, Wu J. One–step synthesis of nitrogen–doped ZnO nanocrystallites and their properties. *Appl Sur Sci*. 2009;255(11):5656–5661.

40. El–Kemary M, El–Shamy H, El–Mehasseb I. Photocatalytic degradation of ciprofloxacin drug in water using ZnO nanoparticles. *J lumen*. 2010;130(12):2327–2331.

41. Pouretedal HR, Marzihe H. Bleaching Kinetic and Mechanism Study of Congo Red Catalyzed by ZrO2 Nanoparticles Prepared by Using a Simple Precipitation Method. *Acta Chim Slov*. 2010;57(2):415–423.

42. Ranjit KT, Willner I, Bossmann SH, et al. Lanthanide oxide doped $TiO_2$ photocatalysis: Novel photocatalysis for enhanced degradation of p–chlorophenoxylacetic acid. *Environ Sci Technol.* 2001;35(7):1544–1549.

43. Daneshvar N, Aber S, Seyed Dorraji MS, et al. Preparation and Investigation of Photocatalytic Properties of ZnO Nanocrystals: Effect of operational parameters and kinetic study. *Int J Chem Biomol Engg*. 2008;1:24–29.

44. Xiao Q, Zhang J, Xiao C, et al. Photocatalytic decolorization of methylene blue over $Zn_{1-x}Co_xO$ under visible light irradiation. *Mat Sci Engineering*. 2007;142:121–125.

45. Rao AN, Sivasankar B, Sadasivam V. Kinetic study on the photocatalytic degradation of salicylic acid using ZnO catalyst. *J Hazard Mater*. 2009;166(2–3):1357–1361.

46. Gaya UI, Abdullah AH, Zainal Z, et al. Photocatalytic treatment of 4–chlorophenol in aqueous ZnO suspensions: Intermediates, influence of dosage and inorganic anions. *J Hazard Mater.* 2009;168(1):57–63.